Phonon-Induced Quantum Magnetic Deflagration in Mn$_{12}$

A. Hernández-Mínguez,[1] F. Macià,[1] J. M. Hernandez,[1] J. Tejada,[1] and P. V. Santos[2]

^{1}*Departament de Física Fonamental, Facultat de Física, Universitat de Barcelona*
Avda. Diagonal 647, Planta 4, Edifici nou, 08028 Barcelona, Spain
^{2}*Paul-Drude-Institut für Festkörperelektronik, Hausvogteiplatz, 5-7, 10117 Berlin*
(Dated: February 6, 2008)

A comprehensive set of experiments on the effect of high-frequency surface acoustic waves, SAWs, in the spin relaxation in Mn$_{12}$-acetate is presented. We have studied the quantum magnetic deflagration induced by SAWs under various experimental conditions extending the data shown in a very recent paper [A. Hernández-Mínguez *et. al.*, Phys. Rev. Lett. **95**, 217205 (2005)]. We have focused our study on the dependence of both the ignition time and the propagation speed of the magnetic avalanches on the frequency, amplitude, and duration of the SAW pulses in experiments performed under different temperatures and external magnetic fields.

I. INTRODUCTION

Molecular nanomagnets are well-defined discrete molecules consisting of several transition metal ions interacting through organic and/or inorganic ligands. The so called single molecule magnets, SMMs, are characterized by two energy scales: i) the strong exchange interactions between metal ions within a molecule, and ii) an anisotropic spin-orbit coupling that results in pronounced magnetic anisotropy. Some of these SMMs have large spin (S) values as well as a high energy anisotropy barrier to prevent spontaneous magnetization reversal at low temperatures.[1] These well characterized objects have an intermediate size between microscale and macroscale and thus allow for the study of phenomena at the border between macroscopic quantum tunnelling and the conventional quantum mechanics of spin. The first unambiguous evidence for resonant magnetization tunnelling in molecular magnets came from the stepwise magnetic hysteresis experiments at different temperatures performed on a Mn$_{12}$-acetate sample, which has $S = 10$ and an anisotropy barrier height $U = DS_z^2 = 60$ K.[2] Since then, numerous experiments have been performed on several SMMs demonstrating the existence of very interesting phenomena, which are well accounted for by theoretical calculations. For a review see Refs. 3,4,5.

To understand the physics of the SMMs, let us assume the simplest Hamiltonian with the magnetic field applied parallel to the easy anisotropy axis:

$$\mathcal{H} = -DS_z^2 - H_zS_z \qquad (1)$$

This Hamiltonian yields pairs of degenerate levels for fields $H_z = nD$ with $n = 0, 1, \ldots, S$. When all molecules occupy the spin states with a negative magnetic quantum number m, the sample is said to be magnetized in the negative direction. By applying a magnetic field in the positive z direction, the molecules eventually relax to the spin states with positive m. This process may occur via thermal transitions over the energy barrier or through quantum tunnelling between the states on different sides of the energy barrier. The tunnelling adds to the thermal activation when the levels at the two sides of the barrier are on resonance, that is at $H_z = nD$. To account for tunnelling, one must include additional terms in the spin Hamiltonian, which do not commute with S_z. These terms may be associated with transverse anisotropy, like quadratic and higher-order terms in S_x and S_y or the transversal Zeeman energy term $-H_xS_x$.

From the experimental point of view, there are two approaches to study spin tunnelling: by 1) measuring the magnetic relaxation at fixed temperature and magnetic field or by 2) sweeping the magnetic field through the resonant field and detecting the fraction of molecules, η, that change their magnetic moment. η depends on the overlap of the wave functions of the resonant spin states at the two sides of the barrier, which defines the tunnelling splitting, Δ, as well as on the sweep rate of the magnetic field energy, v, according to the expression

$$\eta = 1 - \exp(-\frac{\pi\Delta^2}{2\hbar v}) \qquad (2)$$

Since the 1990s,[6,7] it has been known that for fast sweeping rates, the magnetic reversal in large crystals takes place in a short time scale (typically less than 1 ms) through so-called magnetic avalanches. In this process, the initial relaxation of the magnetization towards the direction of the magnetic field results in the release of heat that further accelerates the magnetic relaxation. Recent local magnetic measurements on Mn$_{12}$-acetate crystals have demonstrated that during an avalanche the magnetization reversal occurs inside a narrow interface that propagates through the crystal at a constant speed of a few meters per second.[8] This phenomenon has been named "magnetic deflagration" because of its parallelism to classical chemical deflagration. Deflagration is a subsonic combustion that propagates through thermal conductivity (a steady flame heats the next layer of cold material and ignites it). Classically, combustion describes the exothermic chemical reaction between a substance and a gas (usually O$_2$). The gas oxidize the substance (the fuel), leading to heat release. During magnetic de-
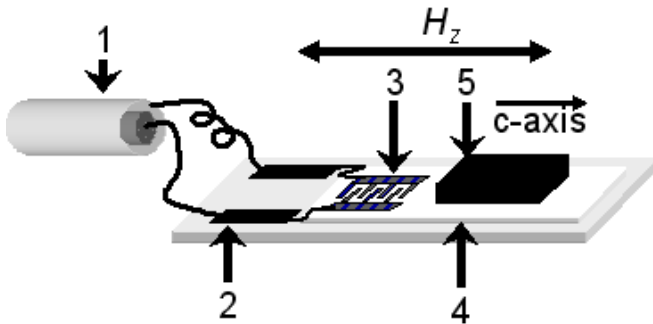
FIG. 1: Experimental setup. 1-coaxial cable; 2-conducting stripes; 3-interdigital transducers (IDT); 4-LiNbO$_3$ substrate; 5-Mn$_{12}$ crystal. The c-axis of the Mn$_{12}$ crystal is oriented parallel to the applied magnetic field H_z.

flagration, the magnetic field "oxidizes" spins originally in a meta-stable state and makes them flip. The released heat then feedbacks the magnetization reversal process.

Recently, a novel method for the controlled ignition of avalanches at constant magnetic field by means of surface acoustic waves, SAWs, has been reported.[9] These acoustomagnetic experiments are performed by using hybrid piezoelectric interdigital transducers deposited on a LiNbO$_3$ substrate, with the Mn$_{12}$ single crystals directly glued onto the piezoelectric.[9,10] The investigations have clearly shown that the propagation speed of the avalanches exhibits maxima for magnetic fields corresponding to the tunnelling resonances of Mn$_{12}$-acetate. The results suggest, therefore, a novel physical phenomenon: deflagration assisted by quantum tunnelling. In this paper, we study these well-controlled ignited magnetic avalanches assisted by spin tunnelling in Mn$_{12}$-acetate under various experimental conditions.

II. EXPERIMENTAL SET UP

The acoustomagnetic experiments were performed by using hybrid piezoelectric interdigital transducers (IDT) deposited on 128 YX-cut LiNbO$_3$ substrates[11] with dimensions $4 \times 12 \times 1$ mm^3. Several single crystals of Mn$_{12}$-acetate with average dimensions of $2 \times .5 \times .5$ mm^3 were studied. Each crystal was measured independently. The sample was glued directly onto the IDT using a commercial silicon grease. The microwaves for the SAW generation were transported to the transducers by coaxial cables (cf. Fig. 1). Experiments have been carried out using a commercial rf-SQUID Quantum Design magnetometer at temperatures between 2 and 2.7 K.

The frequency response of the IDTs was measured using an Agilent network analyzer. The frequency dependence of the reflection coefficient S_{11}, displayed in Fig. 2(a), shows that the coaxial cables introduce an attenuation smaller than 10 dB. The IDT generates SAWs

at multiple harmonics of the fundamental frequency of 111 MHz up to a maximum frequency of approximately 1.5 GHz. Next to the S_{11} determination, we also measured the frequency dependence of the magnetization changes induced by the SAWs in the superparamagnetic regime of Mn$_{12}$ (i.e., for temperatures > 3 K). In this case, the microwave pulses used to excite the IDT were generated by a commercial Agilent signal generator, which allows the selection of the shape, duration, and energy of the pulses in the frequency range between 250 kHz to 4 GHz. Most of the experiments were performed using rectangular microwave pulses of duration 10 μs - 10 ms. Fast magnetization measurements (time resolution of 1 μs) were carried out at constant temperature and magnetic field by continuously recording the voltage variation detected by the rf-SQUID. The negative magnetization changes ($-\Delta M$, see Fig. 2b) show peaks at the resonance frequencies of S_{11}, thus clearly demonstrating that they are induced by the acoustic field. The magnitude of the magnetization variation for each peak depends on how much acoustic energy is absorbed by the Mn$_{12}$ single crystal. During the experiments, the temperature of the IDT attached to the sample and the temperature of the helium gas that provided heat exchange were independently monitored.[10]

To study magnetic avalanches, we first saturated the sample magnetization at -2 T (i.e., below the blocking temperature) and then swept the magnetic field at a constant rate of 300 Oe/s up to a predefined value H. A few seconds later, we applied a rectangular microwave pulse with well-controlled frequency, energy, and duration to excite the SAWs and trigger the magnetic avalanche. These experiments have established a new method for igniting magnetization avalanches in molecular magnets with total control of the magnetic field and initial temperature. Furthermore, by varying the frequency, duration, and nominal power of the pulse we have been able to study the dynamics of the avalanche ignition process.

III. DISCUSSION

A. Time evolution of the avalanches

Figure 3 shows the time evolution of the magnetization during avalanches ignited at $T = 2$ K with SAWs pulses of $t_p = 5$ ms at different magnetic fields. As the whole experiment is performed in a time on the order of a few seconds (i.e., much shorter than the relaxation time in the absence of acoustic excitation), it can be carried out at any temperature below the blocking temperature $T_B = 3$ K. From the magnetic point of view, the important experimental fact is that since the magnetization is measured with a resolution time of 1 μs, we have been able to detect three different stages during magnetization reversal:
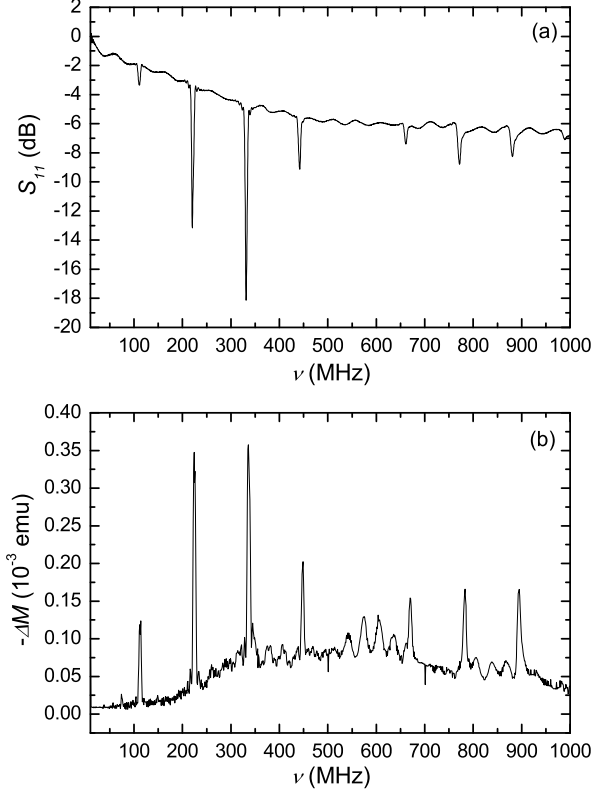
1. The first stage corresponds to the time elapsed be-

FIG. 2: (a) Reflection coefficient, S_{11}, of the $LiNbO_3/Mn_{12}$ hybrids (including the effects of the coaxial assembly used to feed the microwave power) and (b) magnetization variation measured by the magnetometer as a function of the frequency of the microwave pulses sent to the interdigital transducer (IDT). The temperature and applied magnetic field are $T = 6$ K and $H = 1$ T, respectively.

FIG. 3: Time evolution of the magnetization, M, for different magnetic fields at $T = 2$ K. The magnetization is normalized to the total magnetization change during the avalanche, M_{aval}. The duration of the SAWs pulse is $t_p = 5$ ms and the frequency is $\nu = 449$ MHz. $t = 0$ ms corresponds to the instant at which the microwave pulse is applied. The results show that the rate of change of the magnetization peaks at the resonant fields of $H = 4600$ Oe and $H = 9200$ Oe.

tween the application of the microwave pulse and the first detection of magnetization changes. During this time, the SAWs thermalize and the magnetization reversal process nucleates within a small region of the Mn_{12} crystal. To define this nucleation time, we have adopted the criterium that it corresponds to the time interval between the application of the SAWs pulse and the detection of the first magnetization change.

2. The second stage corresponds to the time interval between nucleation and the formation of a stable deflagration front propagating with constant velocity through the crystal.[8] During this time, the nucleation bubble containing reversed spins becomes larger and larger until a steady interface is formed and it propagates along the sample (the "flame" in magnetic deflagration). The heat energy liberated during spin reversal corresponds to the Zeeman energy $\Delta E = g\mu_B H_z \Delta S$ per spin. The temperature
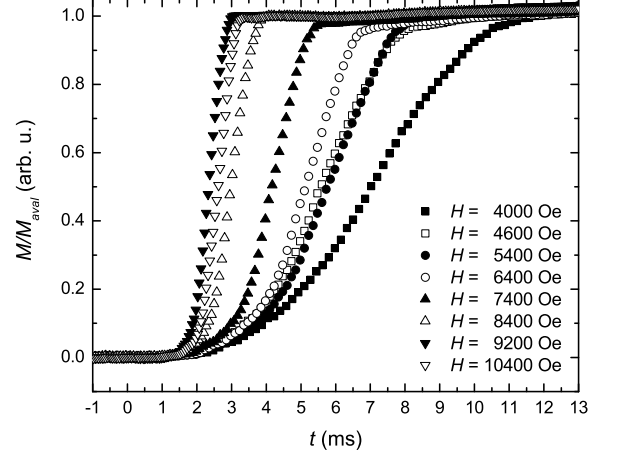
increase induced by the spin reversal leads to the expansion of the nucleation bubble across the width of the Mn_{12} crystal (cf. Fig. 1). In contrast to the subsequent steady-state propagation along the c-axis, this propagation of the front flame depends on the geometry of the crystal and on its magnetic history. For instance, the time to reach that flame will depend on the width of the sample. We call the *ignition time*, t_{ign}, the total duration of these two first steps.

3. The third stage corresponds to the so-called magnetic deflagration, where the flame propagates at constant velocity along the c-axis of the Mn_{12} single crystal. During this time, the rate of magnetization variation is constant and the flame front has a finite width δ. Contrary to the previous stage, the temperature remains constant at value T_f considerably greater than those achieved during the flame formation.

Figure 4(a) shows the velocity $v = l/\Delta t$ of the deflagration front deduced from the magnetization data displayed in Fig. 3. Here, l is the length of the crystal and the avalanche time, Δt, is defined as the time needed by the magnetization to change between the 20% and the 80% of the total variation, M_{aval}. The velocity v increases with the applied magnetic field and presents peaks at the resonant field values. The dependence on magnetic field is well-fitted (see solid line in Fig. 4(a)) by the law:[8]

$$v = \sqrt{\frac{\kappa}{\tau_0}} \exp\left[-\frac{U(H)}{2k_B T_f}\right] \qquad (3)$$

where κ is the thermal diffusivity. $U(H)$, τ_0 and T_f are, respectively, the energy barrier, the attempt frequency, and the temperature of the "flame", which are related to the "chemical reaction time" τ by the expression $\tau = \tau_0 \exp[U(H)/k_B T_f]$. In the case of Mn_{12}, $\kappa \sim 10^{-5}\ m^2/s$, $\tau_0 \sim 10^{-7}$ s, and the field dependence of the energy barrier, $U(H)$, is well known.[7,12] The temperature of the flame increases linearly with magnetic field. According to the fitting, the temperature of the flame front is about 6.8 K for H =4600 Oe, and increases to 10.9 K for H =9200 Oe.

Figure. 4b shows the dependence of the ignition time (i.e., the time delay between the application of the microwave pulse and the observation of a steady flame front) on magnetic field. The ignition time decreases with increasing magnetic field, and shows minima at the resonant fields. The later are a consequence of the enhanced spin reversal probability at the resonant fields. In other words, the ignition time reproduces the dependence of the effective barrier height for magnetic transitions on the magnetic field.

FIG. 4: (a) Velocity and (b) ignition time (t_{ign}) of the deflagration front as a function of magnetic field recorded at $T = 2$ K by using $t_p = 5$ ms SAWs pulses with a frequency $\nu = 449$ MHz. The vertical dotted lines mark the resonant field values. The solid line displays a fit to Eq. 3.

B. The applied acoustic energy

To analyze the dependence of the avalanches on the acoustic energy supplied by the SAWs, we applied SAWs pulses of different durations, t_p, and power, P, and the time evolution of the magnetization for magnetic fields at and out of resonance was recorded.

A very interesting point is that, at a given field and temperature, there is a minimum value for the acoustic energy Pt_p required to trigger the avalanche. As illustrated in Fig. 5(a) and Fig. 5(b), this threshold energy can be surpassed by varying either the amplitude or the duration of the acoustic pulses. The acoustic energy supplied by the piezoelectric in excess of the threshold energy for ignition has no further influence on the avalanche dynamics, which becomes determined only by temperature and by the amplitude of the magnetic field.

These results can be easily understood if we consider that the threshold energy is the minimal energy required to create the initial bubble of reversed spins. Once the nucleation process is overcome, the energy released by spin reversal is much greater than the acoustic energy delivered by the SAWs. This process is analogous to the ignition of a combustion process: the material to be burned has to be externally heated only until the combustion begins. After that, the amount of energy released by the exothermic reaction is large enough to maintain the combustion front propagating through the material.
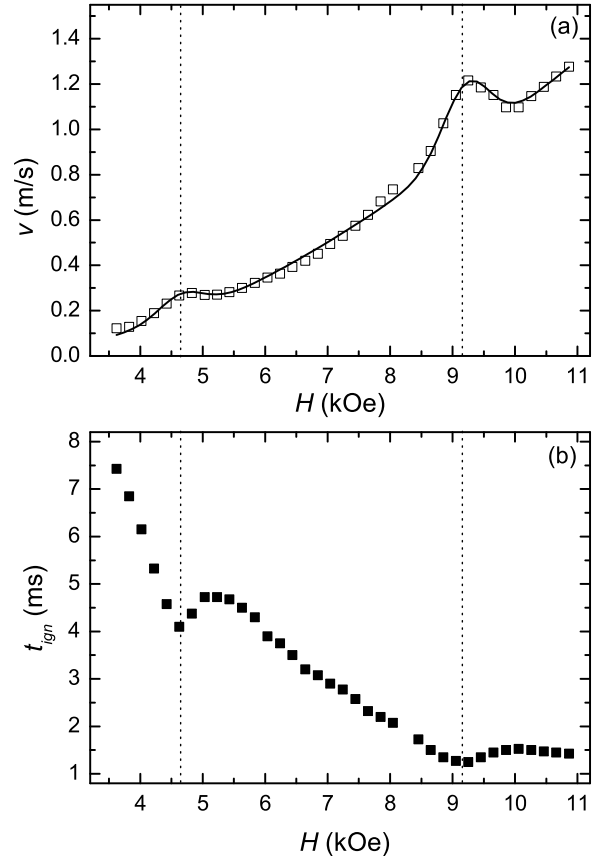
C. Temperature dependence

In order to study the dependence of the deflagration on the initial amount of reversed spins, we have produced magnetic avalanches at different temperatures and magnetic fields by applying acoustic pulses of fixed duration and amplitude. Figure 6 illustrates the typical behavior found at low temperatures (i.e., below 2.3 K). Under these conditions, the ignition time is temperature independent and decreases exponentially with applied magnetic field, with minima at the resonant field values.

Nevertheless, as the blocking temperature is approached, the ignition time becomes sensitive not only to the magnetic field but also to temperature. In particular, the features associated with the second and third resonances (at $H = 9.5$ kOe and $H = 13.5$ kOe, respectively) change from minima in the t_{ign} traces recorded at low temperatures ($T < 2.3$ K) to maxima in traces measured above 2.3 K. At first sight, one should attribute this be-

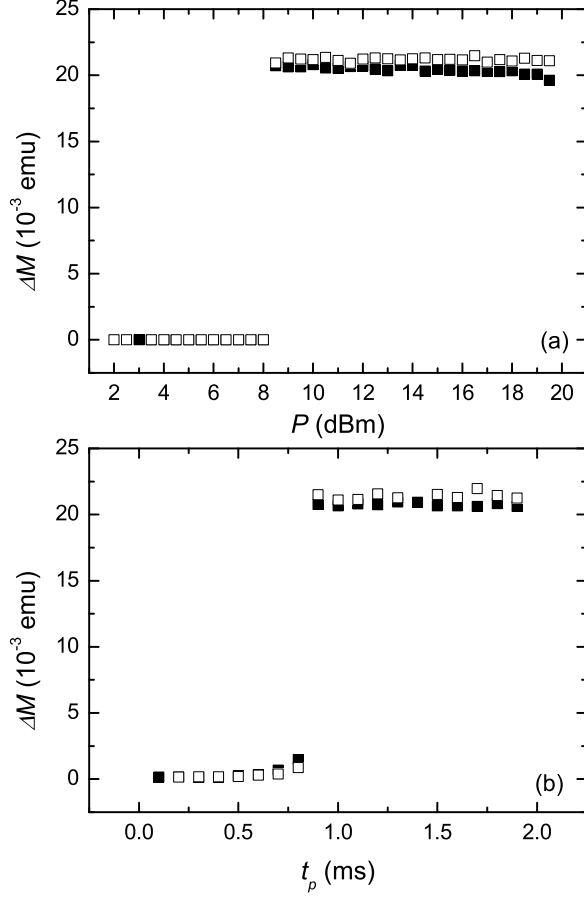FIG. 5: Dependence of magnetization changes during the avalanche on the (a) power (P, recorded for $t_p = 1$ ms) and (b) duration (t_p, recorded for for $P = 20$ dBm) of the SAWs pulses. The measurements were carried out at $T = 2$ K under magnetic fields of $H = 8800$ Oe (solid squares) and $H = 11000$ Oe (open squares).

FIG. 6: Ignition time versus applied magnetic field, H, for different temperatures. The duration of the pulse and frequency are $t_p = 10$ ms, $\nu = 224$ MHz. The inset shows the magnitude of the avalanche for different temperatures and magnetic fields: $H = 4800$ Oe (solid squares), $H = 6400$ Oe (open squares), $H = 9200$ Oe (solid circles), $H = 11000$ Oe (open circles), $H = 14000$ Oe (solid triangles).

havior to the enhanced relaxation that must occur at the resonant fields before the SAWs pulse is applied: since the concentration of metastable spins reduces, it takes longer to create the nucleation bubble required to launch the front flame. In fact, the total magnetization change during the avalanche, M_{aval}, decreases slightly with temperature at low magnetic fields, as indicated in the inset of Fig. 6. However, at high fields and temperatures above 2.3 K, M_{aval} presents an anomalous behavior, which has been consistently observed in several crystals. This behavior is presently not understood and makes unclear the relationship between t_{ign} and the initial magnetic state of the sample in this temperature range.

Figure. 7 shows the time evolution of the magnetization for avalanches ignited at different temperatures under a fixed magnetic field $H = 8$ kOe. Like the ignition time, the velocity of the avalanche depends weakly on the
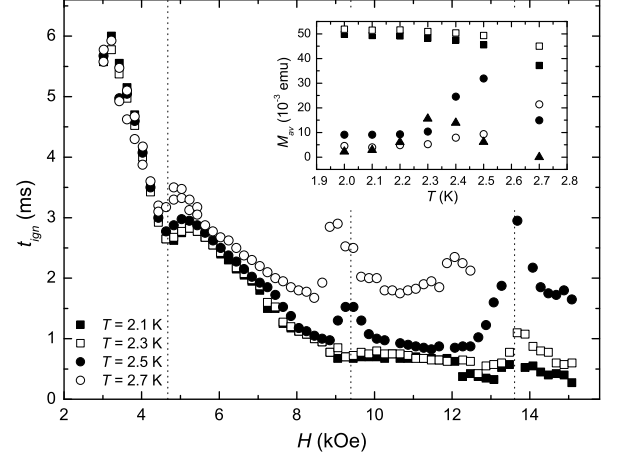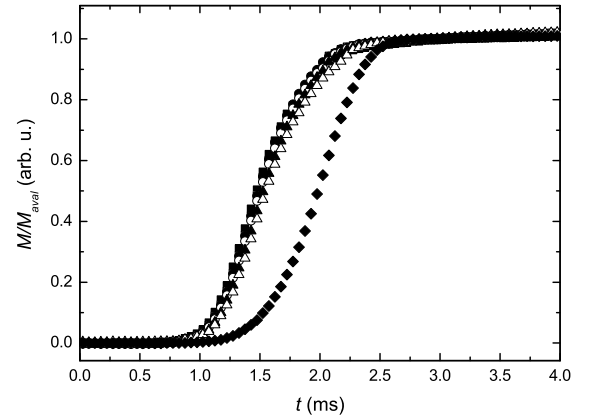

FIG. 7: Time evolution of magnetization for different temperatures under an applied field $H = 8000$ Oe. The values of the initial temperature are: $T = 2.0$ K (solid squares), $T = 2.1$ K (open squares), $T = 2.2$ K (solid circles), $T = 2.3$ K (open circles), $T = 2.4$ K (solid triangles), $T = 2.5$ K (open triangles), $T = 2.7$ K (solid rhombus).

temperature for low magnetic fields, but slowers down at high fields and temperatures.

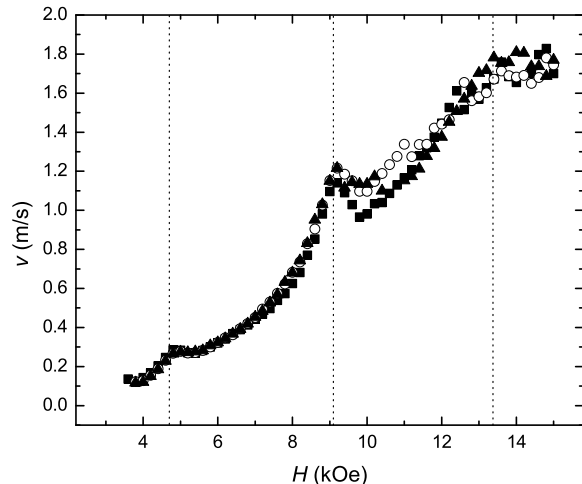FIG. 8: Velocity of the flame front, v, versus applied magnetic field, H, for different SAWs frequencies. The temperature and SAWs pulse duration are $T = 2$ K and $t_p = 5$ ms, respectively. The SAWs frequencies and powers are: $\nu = 224$ MHz and $P = 13.7$ dBm (solid squares); $\nu = 449$ MHz and $P = 15.2$ dBm (open circles); $\nu = 895$ MHz and $P = 20$ dBm (solid triangles).
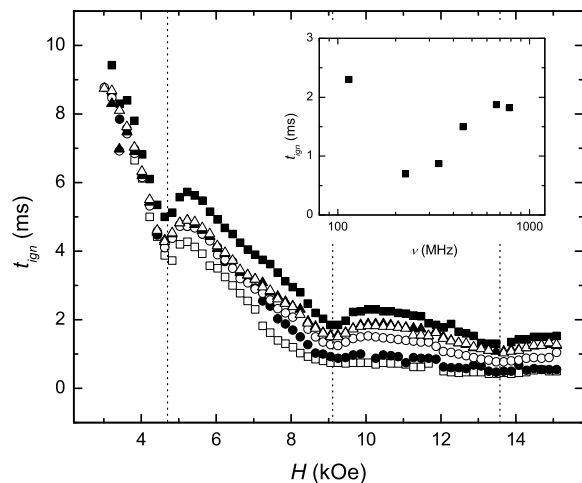

FIG. 9: Ignition time (t_{ign}) versus applied magnetic field, H, and different frequencies of the SAWs. The temperature is $T = 2.1$ K and $t_p = 10$ ms. The values of frequency are: $\nu = 114$ MHz (solid squares), $\nu = 225$ MHz (open squares), $\nu = 336$ MHz (solid circles), $\nu = 449$ MHz (open circles), $\nu = 671$ MHz (solid triangles) and $\nu = 783$ MHz (open triangles). The inset shows the ignition time for different frequencies at $H = 10200$ Oe.

D. Dependence on SAWs frequency

To study the effect of the SAWs frequency on the magnetic avalanches, it is necessary to ensure that, for each frequency, we couple the same amount of acoustic energy to the Mn_{12} crystals. For that purpose, we fixed the duration t_p of the SAWs pulses and selected their amplitude in order to produce the same magnetization variation when the sample is in the superparamagnetic regime. The results are shown in Figs. 8 and 9. As expected, the propagation velocity (Fig. 8) is essentially independent of the frequency of the SAWs, since it is primarily determined by the internal energy liberated during spin reversal. In contrast, the ignition time (Fig. 9), which depends on the external energy supplied by the SAWs, shows a strong frequency dependence. Furthermore, for each magnetic field, the ignition time shows a non-monotonic behavior with frequency, with a minimum at 225 MHz.

IV. CONCLUSION

We have investigated the dynamics of magnetic avalanches induced by acoustic waves in Mn_{12} crystals. The magnetic avalanche becomes a fully deterministic process under acoustic excitation. When the acoustic power exceeds the threshold for the nucleation of the avalanche process, the avalanche dynamics can, therefore, be investigated for different values of the magnetic field and temperature. Well below the blocking temperature, the velocity of the deflagration front of reversing magnetization and the ignition time do only depend on the applied magnetic field. The ignition time depends also on the frequency of the SAWs.

[1] R. Sessoli, D. Gatteschi, A. Caneschi, and M. A. Novak, Nature (London) **365**, 141 (1993).

[2] J. R. Friedman, M. P. Sarachik, J. Tejada, and R. Ziolo,

Phys. Rev. Lett. **76**, 3830 (1996).

[3] D. Gatteschi and R. Sessoli, Angew. Chem. Int. Ed. **42**, 268 (2003).

[4] J. R. Friedman, in *Exploring the Quantum/Classical Frontier: Recent Advances in Macroscopic Quantum Phenomena*, edited by J. R. Friedman and S. Han (Nova, Hauppauge, NY, 2003), p. 179.

[5] E. del Barco, A. D. Kent, S. Hill, J. M. North, N. S. Dalal, E. M. Rumberger, D. N. Hendrickson, N. Chakov, and G. Christou, J. Low Temp. Phys. **140**, 119 (2005).

[6] F. Fominaya, J. Villain, P. Gandit, J. Chaussy, and A. Caneschi, Phys. Rev. Lett. **79**, 1126 (1997).

[7] E. del Barco, J. M. Hernandez, M. Sales, J. Tejada, H. Rakoto, J. M. Broto, and E. M. Chudnovsky, Phys. Rev. B **60**, 11898 (1999).

[8] Y. Suzuki, M. P. Sarachik, E. M. Chudnovsky, S. McHugh, R. Gonzalez-Rubio, N. Avraham, Y. Myasoedov, E. Zeldov, H. Shtrikman, N. E. Chakov, and G. Christou, Phys. Rev. Lett. **95**, 147201 (2005).

[9] A. Hernández-Mínguez, J. M. Hernandez, F. Macià, A. García-Santiago, J. Tejada, and P. V. Santos, Phys. Rev. Lett. **95**, 217205 (2005).

[10] J. M. Hernandez, P. V. Santos, F. Macià, A. García-Santiago, and J. Tejada, Appl. Phys. Lett. **88**, 012503 (2006).

[11] K. Yamanouchi, C. H. S. Lee, K. Yamamoto, T. Meguro, and H. Odagawa (IEEE, New York, 1992), p. 139.

[12] M. Sales, J. M. Hernandez, J. Tejada, and J. L. Martínez, Phys. Rev. B **60**, 14557 (1999).